Canyi Huang[1, 2],
Lina Cui[1, 2],
Hong Xia[3],
Yiping Qiu[4],
Qing-Qing Ni[1, 3,*]

# Influence of Crimp and Inter-Yarn Friction on the Mechanical Properties of Woven Fabric under Uniaxial/Biaxial Tensile Loading

**DOI:** 10.5604/01.3001.0014.3797

[1] Quanzhou Normal University, College of Textiles and Apparel, Quanzhou 362000, China

[2] Shinshu University, Interdisciplinary Graduate School of Science and Technology, Ueda 386-8567, Japan

[3] Shinshu University, Institute for Fiber Enginnering, Ueda 386-8567, Japan,
* e-mail: niqq@shinshu-u.ac.jp

[4] Donghua University, College of Textiles, Department of High-Tech Textiles, Shanghai 201620, China

**Abstract**
*In the present research, a physical-geometric-feature of continuous yarn in a plain woven fabric was created and its FE model was analysed by considering the two key issues of woven fabric, the crimp and inter-yarn friction. The basic parameters of Young's modulus of single yarn and the inter-yarn friction coefficient were investigated for practical fabrics in tensile and pull-out tests. FE analysis indicated that the stress-strain curves of the FE model were effective in evaluating the equivalent modulus of a woven fabric by comparing with a tensile experiment on Twaron CT® Plain Woven Fabric. In addition, a simplified three dimensional model of the unit cell of plain woven fabric (UCPW) was employed to quantitively investigate two important fabric characteristics – the crimp rate of the yarn and inter-yarn friction-to determine their influence on the mechanical properties of the fabrics. Furthermore, we used FE analysis to evaluate how the crimp rate and inter-yarn friction affected the mechanical properties by determining the equivalent modulus of single yarn and UCPW in both uniaxial and biaxial tensile loading. The stresses at representative nodal points and the mechanical interaction between yarns were also investigated from a microscopic perspective, and their deformation mechanisms were also analysed and discussed.*

**Key words:** *finite element analysis (FEA), unit cell of plain woven fabric (UCPW), tensile test, equivalent modulus, crimp, inter-yarn friction.*

## Introduction

Woven fabrics are currently the most often used in clothing, industrial textiles, and even composite manufacture. Therefore, there is a great deal of interest in the prediction of their behavior [1]. The elastic modulus is one of the most important mechanical properties, and is a measure of a material's resistance to elastic deformation. Besides this, finite element analysis (FEA) has frequently been used to simulate and simplify engineering problems. As a result several researchers have used this technique to study elastic tensile properties. Tehrami et al. [2] investigated the tensile behaviour of woven fabrics with various weave patterns using FEA. Lin [3] attempted to predict elastic properties to determine the tensile damage behaviour of a woven fabric. Chen et al. [4] investigated the tensile behaviour of PVC-coated woven membrane materials under uniaxial and biaxial loads. Lin et al. [5] used a modelling approach to study the mechanical behaviour of textile reinforcements; the model simulated combinations of compaction and in-plane shear loading to represent important interactions. Kollegal and Sridharan [6] investigated the mechanical behaviour of plain weave fabric composites under in-plane loading using 3-D finite element analysis in conjunction with a micro-mechanical model. Other related published works [7-12] are also concerned with the various tensile behaviours of woven fabric under different kinds of loading.

Furthermore, the physical properties of woven fabrics – including the crimp rate and inter-yarn or even inter-fibre friction – have a significant influence on their mechanical performance. Tan et al. [13] and Wang et al. [14] demonstrated the influence of the crimp rate on the ballistic properties of woven fabrics. Broughton et al. [15] investigated the effect of inter-fibre friction on the tensile properties of yarns, and demonstrated that inter-fibre friction can be the dominant factor in determining the tensile properties of a ring-spun staple yarn. Wang et al. [16] studied the effect of inter-fibre friction on fibre damage propagation and the ballistic limit of 2-D woven fabrics. Chu et al. [17] showed that greater inter-yarn friction leads to less slippage of the primary yarns at the centre of impact, and prolongs the failure of primary yarns.

Numerous papers have been published on the experimental and numerical simulation of the tensile or other mechanical properties of fabrics, as well as on the influence of the physical properties of woven fabrics such as the crimp rate and inter-yarn friction. However, there are few reports on the determination of the equivalent modulus (note: equivalent modulus in the present study refers to the real performed tensile modulus of fabric as differentiated from the material's original modulus) of woven fabric during tensile loading to investigate how the crimp or inter-yarn friction affects its mechanical properties. Therefore, in the present study, a physical-geometric-feature-based continuous yarn in a plain woven fabric was created and its FE model analyzed by considering the two key issues of a woven fabric – the crimp and inter-yarn friction. The basic parameters of Young's modulus of single yarn and the inter-yarn friction coefficient were investigated for practical fabrics in tensile and pull-out tests. FE analysis indicated that the stress-strain curves of the FE model were effective in evaluating the equivalent modulus of a woven fabric by comparing with a tensile experiment on Twaron CT® Plain Woven Fabric. Furthermore, we used FE analysis to evaluate how the crimp rate and inter-yarn friction affected the mechanical properties by determining the equivalent modulus of single yarn and the unit cell of plain woven fabric (UCPW) in both uniaxial and biaxial tensile loading.

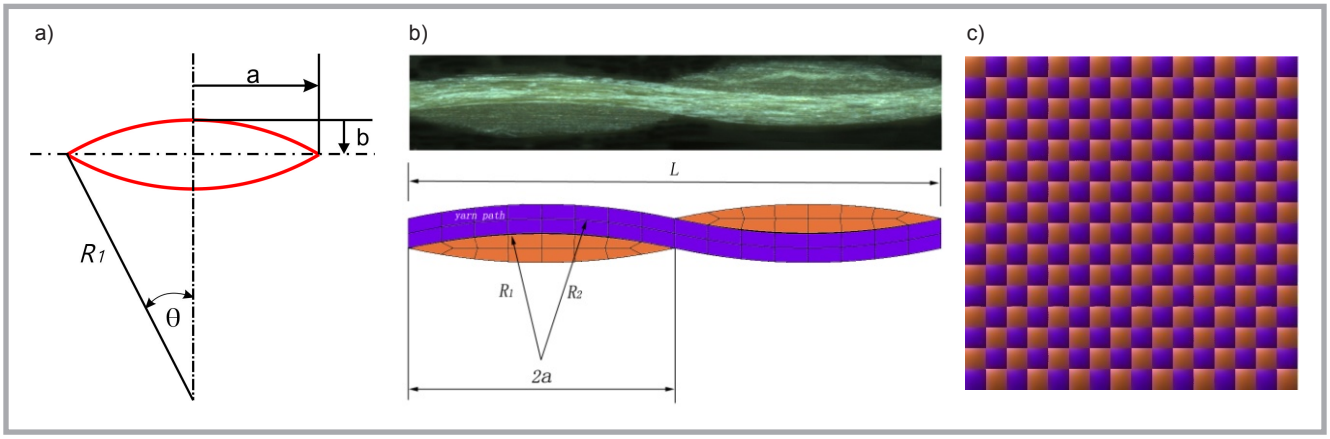


***Figure 1.*** *a) Cross-sectional view of the yarn, b) comparison of the cross-sectional view of the Twaron CT® fabric and geometry model, c) model of Twaron CT® woven fabric.*

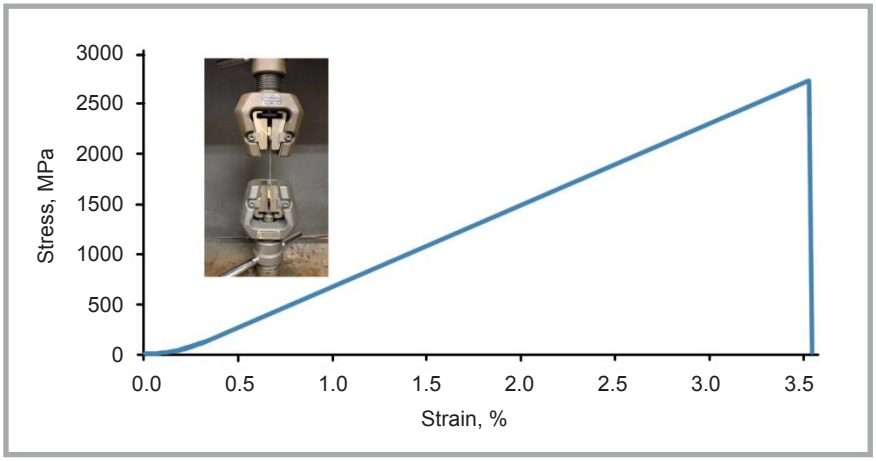


***Figure 2.*** *Tensile experiment results of a single yarn of Twaron CT®.*

***Table 1.*** *Physical parameters of Twaron CT®.*

| Fabric type | Thread density, per cm | Areal density, g/m² | Cross-sectional area of yarn, cm² | Thickness, mm |
|---|---|---|---|---|
| Twaron CT | 11 | 120 | $3.82 \times 10^{-4}$ | 0.2 |

***Table 2.*** *Orthotropic linear-elastic material parameters of a single yarn of Twaron CT® (GPa).*

| $E_{11}$ | $E_{22}$ | $E_{33}$ | $G_{12}$ | $G_{13}$ | $G_{23}$ | $V_1$ | $V_2$ | $V_3$ | TS |
|---|---|---|---|---|---|---|---|---|---|
| 72.63 | 1.13 | 1.13 | 1.04 | 1.04 | 1.04 | 0 | 0 | 0 | 2.764 |

## Model and mechanical parameters of Twaron CT® plain weave fabric

### Geometry modelling of Twaron CT® plain weave fabric

Plain-woven Twaron CT®, a high performance fabric of light weight and high protection application, made by TEIJIN, was employed in this study. This fabric is manufactured using a plain weave of $11 \times 11$ yarns (per cm²), with each yarn consisting of 500 filaments. The bulk density and linear density are 1.44 g/cm³ and 550 dtex, respectively. The cross-sectional area of each yarn was calculated as $3.82 \times 10^{-4}$ cm² by dividing the linear density of the material by its bulk density. We created a fabric model in SolidWorks®, then turned to Ansys® to simulate and analyse the tensile process. The fabric model was created at the yarn level. We implemented the plain weave fabric model in the present study – which takes into account two geometrical aspects, i.e, the cross-sectional shape and path of the yarn – to describe the yarn geometry. Based on a photo of the micro-structural cross-section of Twaron CT® taken by a Yashima® digital microscope YDU-3S, shown in the upper part of ***Figure 1.b***, we assumed that the cross-section of the warp and weft yarns of the fabric was lenticular in shape and consisted of two identical arcs facing each other. In the geometrical model, the cross-section of the yarn remains constant along its length, and the path of the yarn is a curve that represents the yarn waviness through the yarns in the other direction. Cross-sectional views of the yarn and fabric model are provided in ***Figures 1.a*** and ***1.b***. All geometrical parameters can be calculated using the following expressions [18]:

$$L = 2/\text{thread density}, \quad (1)$$

$$b = \text{fabric thickness}/4, \quad (2)$$

$$a = (2bR_1 - b^2)^{1/2} = L/4, \quad (3)$$

$$R_2 = (a^2 + b^2)/2b, \quad (4)$$

$$R_1 = R_2 - b. \quad (5)$$

Where, L is the wavelength of the yarn path, $R_1$ the radius of the arc for the yarn cross-section, $R_2$ the radius of the arc for the yarn path, and a and b are half of the width and half of the height of the yarn cross-section, respectively. ***Figure 1.c*** shows the geometry model of Twaron CT® woven fabric, and ***Table 1*** the physical parameters.

### Basic mechanical properties of Twaron CT®

In this research, an orthotropic linear-elastic material model was employed. The mechanical properties of Twaron CT® are shown in ***Table 2***. $E_{11}$ was obtained by a tensile test of single yarn of Twaron CT®; the tensile result can be seen in ***Figure 2***. The tensile strength (TS) was also calculated as 2.764 GPa. $E_{22}$, $E_{33}$, $G_{12}$, $G_{13}$ and $G_{23}$ were calibrated by taking suggestions from the model by S. Gogineni et al. [19] and C.T. Lim et

al. [20]. Many studies have proved that Poisson's ratios ($V_{12}$, $V_{23}$, $V_{13}$) should be zero and the transverse Young's modulus ($E_2$, $E_3$) and shear modulus ($G_{12}$, $G_{13}$, $G_{23}$) should be very small with respect to the longitudinal Young's modulus $E_1$ to reproduce the thread behaviour of the yarn [21].

### Inter-yarn friction coefficient of Twaron CT®

Inter-yarn friction has been shown to have a significant effect in determining a fabric's mechanical properties; it is also an indispensable parameter in mechanical behaviour simulation. An inter-yarn friction coefficient obtaining method of comparing experiment and simulation results was used in [22].

Firstly, a yarn pull-out test was carried out using a uniaxial tensile test machine (TENSILON®RTF-2350), where individual yarn from Twaron CT® was pulled out with velocity of 0.1mm/min, which was repeated eight times. The effective dimension of the fabric was 70 mm length and 50 mm width. The shear deformation and transverse tension were minimised using a special grip consisting of two U-shaped metallic plates, shown in ***Figure 3.a***.

In addition, simulation was also carried out. Considering the computing cost, a smaller fabric model of Twaron CT® woven fabric with 3 yarns × 11 yarns was created and used to simulate the pull-out process. The displacement of the two short-yarn sides was constrained in all the edges but allowing the spin. The contact between warp and weft yarns was defined as frictional. ***Figure 3.b*** shows the simulation process. In order to examine the effects of the friction, 4 different frictional coefficient (FC) cases were modeled in the test, respectively (FC = 0.1, 0.2, 0.3, 0.4). Numerical simulation results were compared to experimental yarn pull-out curves. Linear regression relation equations for the 1st-4th peak force ( five peaks in total, more details in ***Figure 4***) the FC finalised (the 5th peak was neglected because the error was positive when the experiment test reached the fabric's edge), and the inter-yarn friction coefficient $\mu$ was finalised as 0.3 by averaging the results of each peak. ***Table 3*** shows linear regression relation equations of the peak force and frictional coefficient.

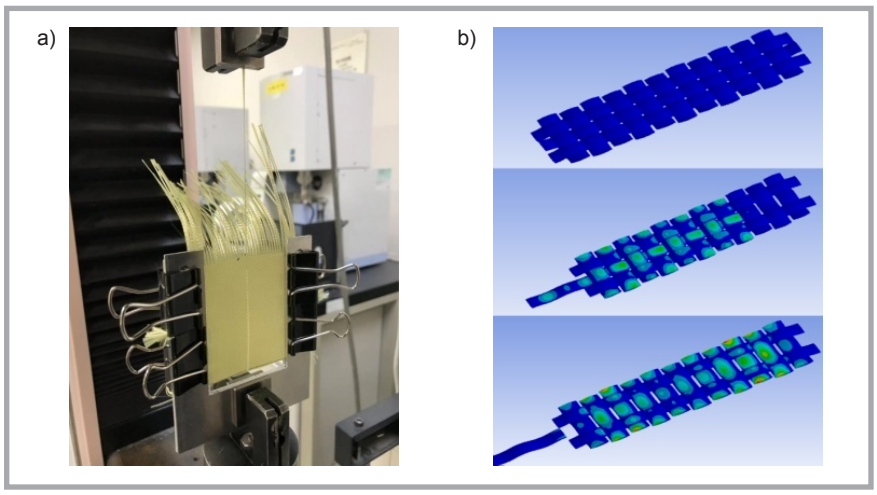


***Figure 3.*** *Pull-out of Twaron CT® woven fabric: a) experiment process, b) simulation process.*

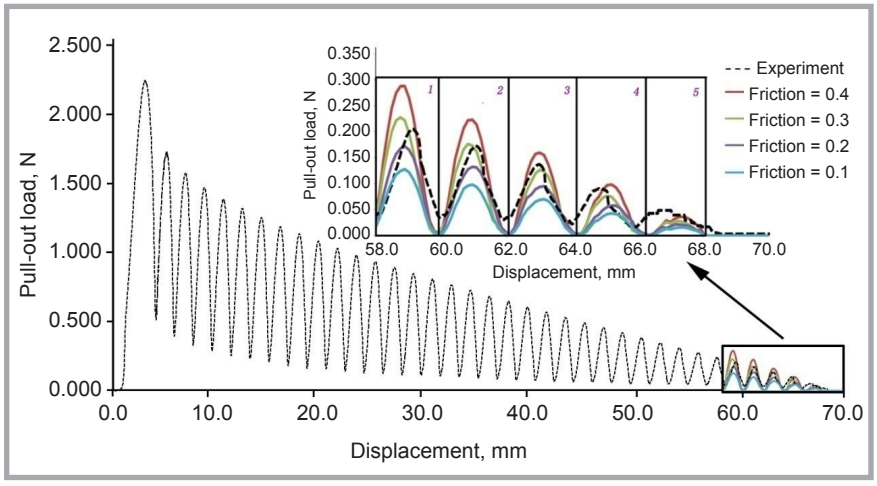


***Figure 4.*** *Comparison of simulation results and experimental result of single yarn pull-out from Twaron CT®.*

## Tensile simulation and experimental verification

Tensile simulation of Twaron CT® was carried out accordingly. The mechanical parameters and inter-yarn frictional coefficient obtained above were applied to the model. The stress-strain curve during the tensile process is depicted as a red dash line in ***Figure 5***, and Young's modulus of the fabric, Es, was calculated as 71.35 GPa when the frictional coefficient was designated to be 0.3. Moreover, a friction coefficient of 0 was also taken into consideration. The stress-strain curve is depicted as a grey dash line in ***Figure 5***. It can obviously be established that the frictional coefficient has an influence on the tensile result, which will be discussed thoroughly in the following content.

In order to validate the effectiveness of the model and simulation process, a tensile test of practical Twaron CT® was carried out. A quasi-static tensile test was done on a 20KN INSTRON machine with a cross-head speed of 1 mm/min.

***Table 3.*** *Linear regression relation equations of the peak force and frictional coefficient for the 1st-4th peaks.*

| | Linear regression relation equation | $R^2$ | Peak force, N | μ |
|---|---|---|---|---|
| 1st peak | F= 0.542μ+ 0.0705 | 0.9955 | 0.291 | 0.275 |
| 2nd peak | F = 0.432μ+ 0.05 | 0.9918 | 0.226 | 0.289 |
| 3rd peak | F = 0.32μ+ 0.0355 | 0.9905 | 0.177 | 0.318 |
| 4th peak | F = 0.256μ+ 0.012 | 0.9893 | 0.123 | 0.334 |

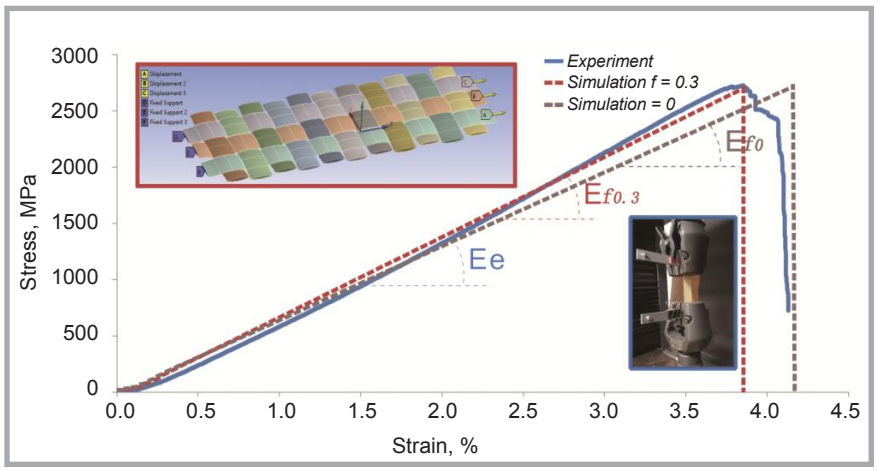


***Figure 5.*** *Comparison of tensile stress-strain curve between the experiment and simulation of Twaron CT® fabric.*

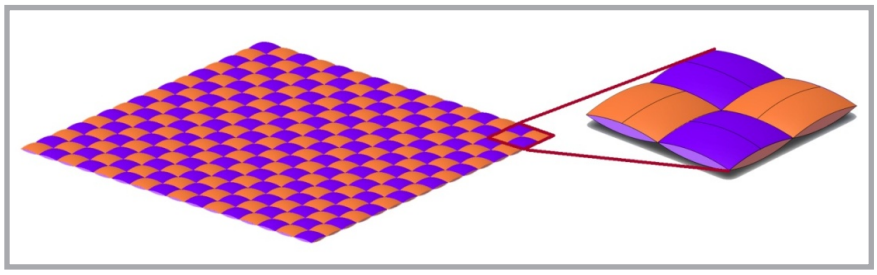

***Figure 6.*** *Schematics of the unit cell of plain woven (UCPW).*

The effective zone of the samples were designated as 2 cm × 10 cm (22 yarns × 110 yarns). Firstly, the samples were cut into oversized ones using special aramid-use scissors, 8 replicates with the length along the warp direction, then extra yarns along the samples' length were removed from both sides in order to ensure that edge defects are minimised and that there is no slip of loaded yarns during the test. Besides this, high-strength epoxy was glued to the ends of the test specimen in order to prevent slippage. A thin aluminum clamp were used for the fixture of the test samples. High resolution photos taken by a camera showed negligible slip between the samples and grips, and no pullout of yarns.

***Table 4.*** *Structural details of fabrics used in finite element (FE) analysis.*

| Model | Thread density, 1/cm | Crimp, % |
|---|---|---|
| 1 | 8.6 | 1.167 |
| 2 | 10.2 | 1.986 |
| 3 | 11 | 2.329 |
| 4 | 11.7 | 3.341 |
| 5 | 12.5 | 4.658 |

A typical stress-strain curve under uniaxial tension was also depicted. As we had what we considered was the tensile property before the fabric's failure, we stopped the tensile experiment before the fabric's complete failure. The curve can be divided into 3 regions: the crimp region, linear pre-peak region and post-peak region. In the crimp region, the stress increases slowly due to the straightening of the undulated yarns in the loading direction with limited yarn stretching. The maximum strain in the crimp region is only 0.0078, which is negligible when compared with the strain at failure. As the strain increases, the fabric exhibits a linear response before failure. The Young's modulus of the fabric is defined by the slope of the stress–strain curve in this region. And the average Young's modulus of the Twaron CT® was calculated as Ee = 73.18GPa.

A comparison of the tensile stress-strain curve between the experiment and simulation can been seen in ***Figure 5***, where the results estimated with a frictional coefficient of 0.3 show great similarity with the experiment results, and the Young's modulus estimated by simulation is approximately 2.5% smaller than the experiment result. As a result, we can conclude that the model used in the simulation can generally reflect the tensile property of real fabric; the model and simulation are proved to be effective.

## Investigation of the influence of crimp and inter-yarn friction on the mechanical properties of plain weave fabric

As we know, different types of fabrics have different crimp and inter-yarn friction coefficients, even ones made of the same material. It is difficult to qualitatively judge their influence on mechanical properties through real material experiments, respectively, whereas FEA can help to deal with these problems due to its powerful parameterisation solution ability. Firstly, five fabric models with the same thickness (0.2 mm) but with different crimp rates were created for FEM analysis. The crimp rate of a woven fabric can be calculated using ***Equation (6)***:

$$\text{Crimp} = \left(8\pi R_2 \frac{\theta}{360} - L\right)/L \times 100\%, \quad (6)$$

Where, θ is half of the central angle (in degrees) of the arc forming the shape of the yarn cross-section R and L can be seen in ***Figure 1***. Structural details of these models are listed in ***Table 4***.

In addition, the present model employed in the test still cost a lot calculation time, as a result of which, a unit cell of plain woven (UCPW) was proposed (see ***Figure 6***) to improve the calculation effectiveness. Tensile simulation results showed there was no difference in the results of the fabric's Young's modulus between the model employed above and the unit cell model, which applied an extra circulated boundary condition in the simulation process [23]. This kind of UCPW model was employed in all the following cases of tests.

### Effect of crimp on the mechanical behaviour of a single yarn

Firstly, before the tensile test on the fabric, we tried to investigate how the crimp impacts the mechanical behaviour of single yarn. Five types of yarns with a different crimp rate were employed in the tensile simulation. An elongation rate of 1% was set in the tensile direction in all the tensile tests, as during linear elastic processes, the level of the elongation rate does not affect the results.

The equivalent tensile modulus, as one of the important indexes of a material's mechanical properties, was calculated from simulation results by obtaining normal stresses and strains in the tensile direction (the z direction in Ansys) when the tensile load was applied. The stresses and strains of all nodal points when the tensile load was applied to the cross-section of the tensile end – denoted by – were excluded from the analysis results. Therefore, the equivalent tensile modulus (Ee) of the yarns during tensile loading could be calculated using the following ***Equation (7)***:

$$Ee = \sum_1^n \sigma / \sum_1^n \varepsilon. \quad (7)$$

The tensile deformation of a single yarn with a crimp of 3.341% is represented in ***Figure 7.a***. The crimped yarn straightened during the tensile process, and the movement of the yarn reveals that both tensile and bending phenomena occurred during the tensile process. The normal stress distribution in the tensile direction is represented in ***Figure 7.b***. The results of the analysis are acceptable because there was no stress concentration. The maximum normal stress was clearly located on both sides of the areas of greatest curvature, as represented by the red and blue areas.

The equivalent modulus for each degree of crimp was calculated, and the decreasing trend in the equivalent modulus was also obtained, as shown in ***Figure 8***. The equivalent tensile moduli of single yarns were obviously smaller than those of the original material (72.63 GPa) at all crimp rates, being inversely proportional to the crimp rate. The equivalent moduli of the yarns dropped from 98.35% to 94.78% of the original modulus when the crimp increased from 1.167% to 4.658%. This means that for the same material with the same original tensile modulus, the degree of crimp resulting from the production process affects the equivalent modulus of the yarn during mechanical loading; the more curved the yarn, the smaller its tensile modulus.

We then carried out a microscopic examination of the stress at the FE nodal points. ***Figure 9*** shows the normal stress distribution in the tensile direction (z) of nodal points through the upper surface of a yarn with a crimp of 3.341%. The nodal points selected are highlighted in violet in the side view of the single yarn model. The schematic of the results represents

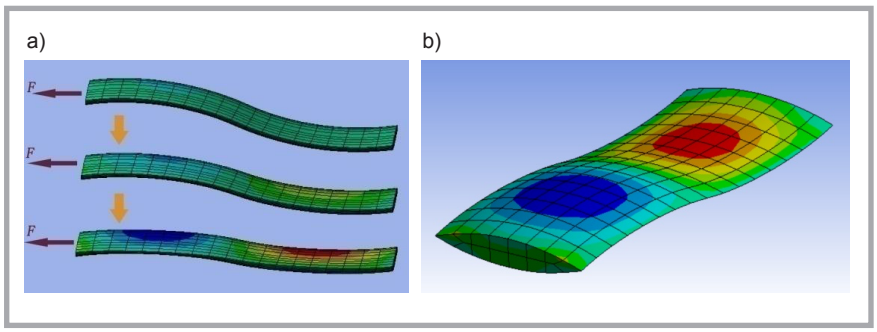


***Figure 7.*** *Schematics of FE tensile characteristics of a single yarn with a crimp of 3.341%: a) tensile deformation process and b) normal stress distribution in the tensile direction.*

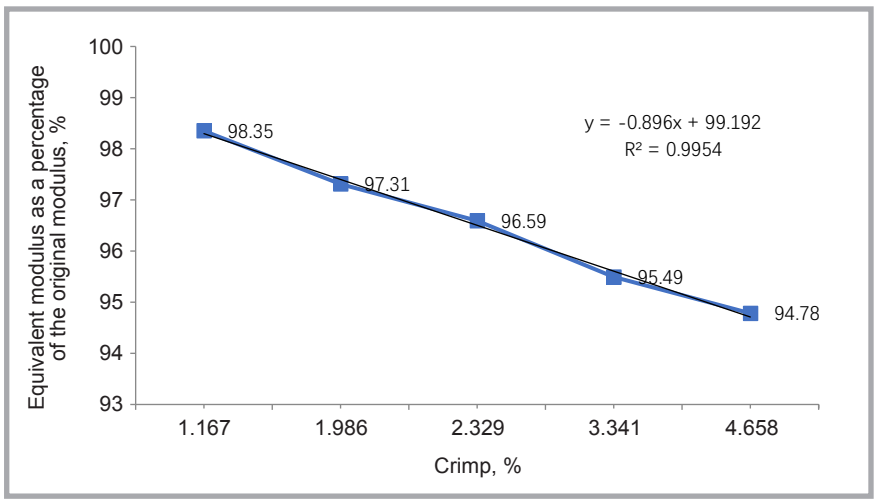


***Figure 8.*** *Equivalent modulus as a percentage of the original modulus versus the crimp rate in a tensile test on a single yarn.*

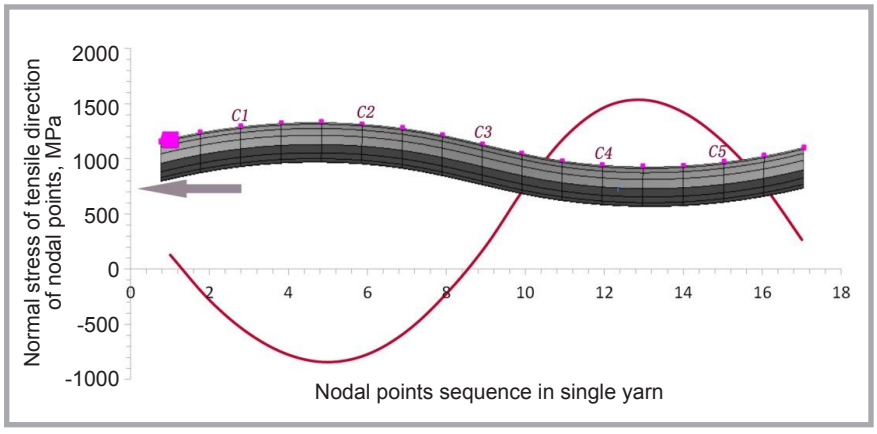


***Figure 9.*** *Normal stress distribution of nodal points in the tensile direction through the upper surface of a yarn with a crimp of 3.341%.*

***Table 5.*** *Comparison of normal stresses (MPa) in the tensile direction at representative nodal points C1-C5 for yarns with various crimp rates.*

| Nodal point | Normal stress, MPa | | |
|---|---|---|---|
| | Crimp 1.167% | Crimp 2.329% | Crimp 4.658% |
| C1 | 592.3 | 589.1 | 585.4 |
| C2 | 790.2 | 783.9 | 771.2 |
| C3 | 288.9 | 258.3 | 211.6 |
| C4 | 1488.9 | 1477.5 | 1465.8 |
| C5 | 1195.3 | 1178.6 | 1156.7 |

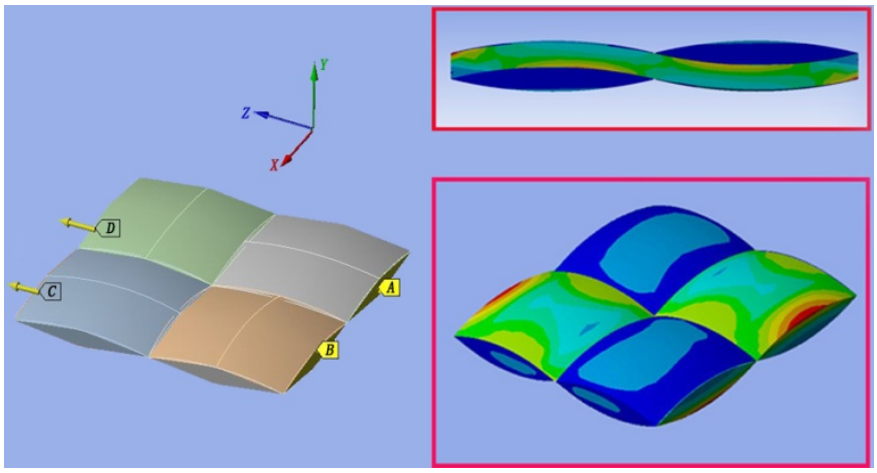


***Figure 10.*** *Schematics of boundary conditions and normal stress distribution in the tensile direction in a uniaxial tensile test on a unit cell of plain woven (UCPW).*

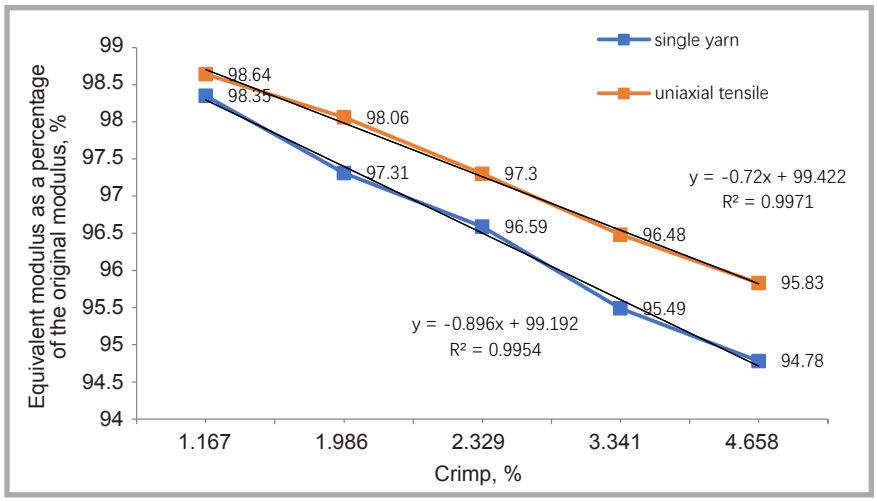


***Figure 11.*** *Comparison of the equivalent modulus as a percentage of the original modulus of a single yarn and UCPW versus the crimp rate in a uniaxial tensile test.*

an approximate trigonometric function curve. The normal stresses at the representative nodal points (C1-C5) in three yarns with different crimp rates are listed in ***Table 5***. The results illustrate that each nodal stress in the tensile direction (in absolute terms) was greater when the degree of crimp was smaller. This result also means that under the same tensile elongation, the yarn with the greatest crimp rate experienced less stress in the tensile direction. We also investigated the deformations of the same nodal points in the perpendicular Y direction (see ***Table 6***). The results illustrate that the deformation of each nodal point in the Y direction was greater when the degree of crimp was larger. Because displacement reduces stress to some extent, during tension, the greater the degree of deformation perpendicular to the direction of tension, the smaller the stress in the direction of tension inside the material. This means that under the same elongation rate, yarns with a greater crimp rate experience greater bending deformation, and unstable dynamic action reduces the tensile stress and strain in the tensile direction, making the yarn easier to stretch than one with a lower crimp rate. Such yarns also have a lower equivalent modulus.

***Table 6.*** *Comparison of deformation (mm) of nodal points C1-C5 in the perpendicular Y direction for yarns with various crimp rates.*

| Nodal point | Crimp 1.167% | Crimp 2.329% | Crimp 4.658% |
|---|---|---|---|
| C1 | 0.137 | 0.158 | 0.169 |
| C2 | 0.118 | 0.134 | 0.143 |
| C3 | 0.064 | 0.078 | 0.086 |
| C4 | 0.019 | 0.026 | 0.032 |
| C5 | 0.006 | 0.009 | 0.0011 |

## Effect of crimp on the mechanical behaviour of woven fabric

### *Uniaxial tensile*

A unit cell of plain woven (UCPW) comprises four contact regions because it is composed of two warp yarns and two weft yarns. These contact regions are responsible for inter-yarn friction, which cannot be negligible in the tensile simulation process. Therefore, a constant frictional coefficient between the contact regions of 0.3 is applied in tests at all crimp levels. A model UCPW comprising yarns with a crimp of 3.341% and applied boundary conditions are represented in ***Figure 10***. Cross-sections A and B represent fixed ends, whereas cross-sections C and D are tensile ends. The cyclic symmetry of the normal stress distribution in the tensile direction owing to the symmetry of the UCPW can also be seen in the lower right schematic surrounded by a red border in ***Figure 10***. The maximum normal stress area is located around the outside rim of the cross-section in the load-bearing yarn. The stress distribution of the cross-section of the UCPW can be seen in the upper right schematic surrounded by a red border. The stress in the load-bearing yarns is greater than in the non-loaded ones.

The equivalent tensile modulus of the UCPW under uniaxial tensile loading demonstrated the same trend as in the single yarn test: a greater crimp resulted in a lower equivalent modulus (***Figure 11***). The equivalent modulus of the UCPW dropped from 98.64% to 95.83% of the original modulus when the crimp increased from 1.167% to 4.658%. It is also clear that the moduli at all levels of crimp were smaller than that of the original material. A comparison of the uniaxial tensile tests on the single yarn and UCPW reveals that the equivalent modulus was greater in the UCPW at all levels of crimp than in the single yarn, which is in accordance with the tensile experiments described above. In addition, the linearly fitted results from the uniaxial tensile tests reveal that crimp had a slightly greater influence on the single yarn than on the UCPW. Furthermore, the difference in the equivalent modulus between the single yarn and the uniaxial

tensile case increased from 0.2% to 1.1% as the crimp increased.

We also investigated the stress between yarns in the cross-section of the UCPW under uniaxial tensile loading. When tensile loading was applied, tensile elongation in yarn A resulted in friction stress on the contact surface (indicated by the red line in the side view in ***Figure 12***) caused by the hindrance of yarns B and C; simultaneously, bending in yarn A resulted in extrusion stress normal to the fabric plane on the contact surface, also due to the hindrance of yarns B and C. ***Figure 12*** shows the stress condition at the central contact nodal point of yarn A. In contrast, in the single yarn test there was no hindering yarn to prevent the elongation and bending of the tensile yarn; so compared with the UCPW, the single yarn was easier to stretch, which explains the difference in the equivalent moduli between the UCPW and single yarn.

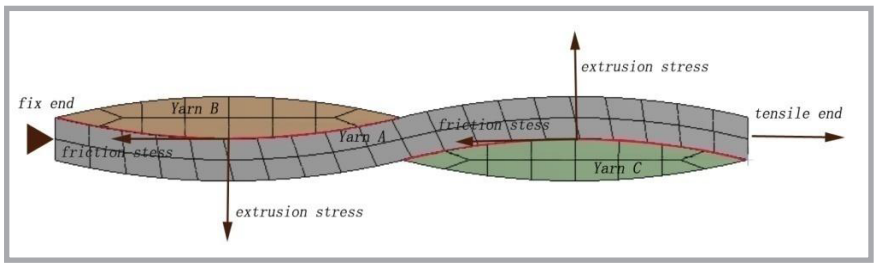


***Figure 12.*** *Stress between yarns in the cross-section of UCPW at the central contact nodal point during uniaxial tensile loading.*

### *Biaxial tensile test*

We also took biaxial tensile tests into consideration. Compared with the uniaxial tensile tests, in the biaxial test we applied tensile loading to yarns in both the warp and weft directions while maintaining an inter-yarn frictional coefficient of 0.3. Cross-sections A, B, C, and D are the fixed ends, and cross-sections E, F, G, and H are the tensile ends (***Figure 13***). In the biaxial test we applied tensile loads to the warp and weft yarns simultaneously at a rate of 1% elongation in both directions. Considering the symmetry of the UCPW, the results for the two directions should be the same. Therefore, the results for either direction are acceptable. The schematic surrounded by the red border in the lower right of ***Figure 13*** also shows the normal stress distribution in a single tensile direction (the schematic represents a view magnified five times). The cyclic symmetry results also reveal that the maximum stress occurred both around the rim of the cross-section and around the cross contact area between the two groups of yarns. Furthermore, the stress was quite evenly distributed between the weft and warp yarns, shown in the schematic surrounded by the red border in the upper right of ***Figure 13***.

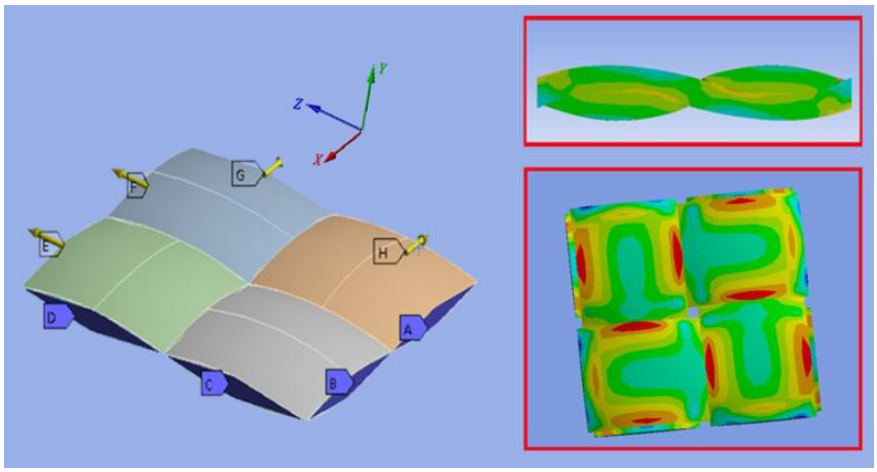


***Figure 13.*** *Schematic of the boundary condition and normal stress distribution in the single tensile direction in UCPW during the biaxial tensile test.*

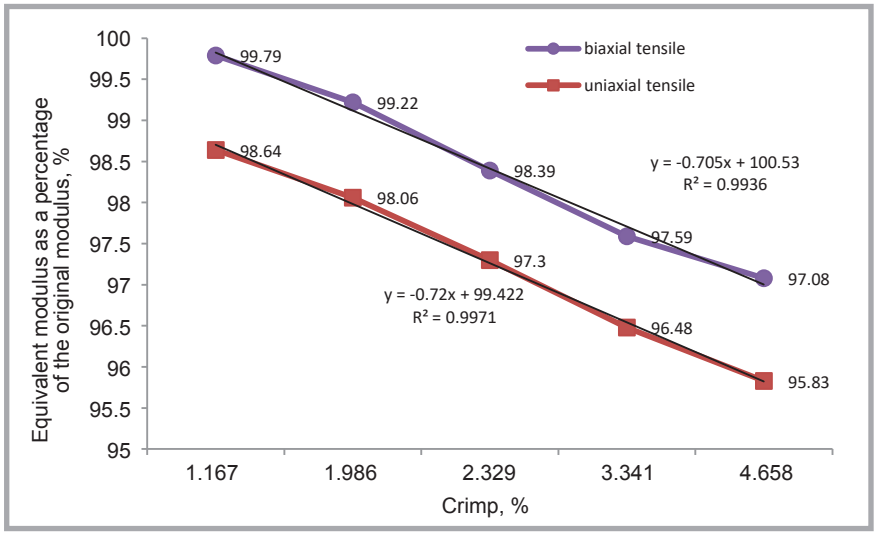


***Figure 14.*** *Comparison of the equivalent modulus as a percentage of the original modulus versus the crimp in UCPW in the uniaxial and biaxial tensile tests.*

***Figure 14*** reveals that the equivalent tensile moduli in UCPWs with different crimps were closer to the modulus of the original material in the biaxial ten-

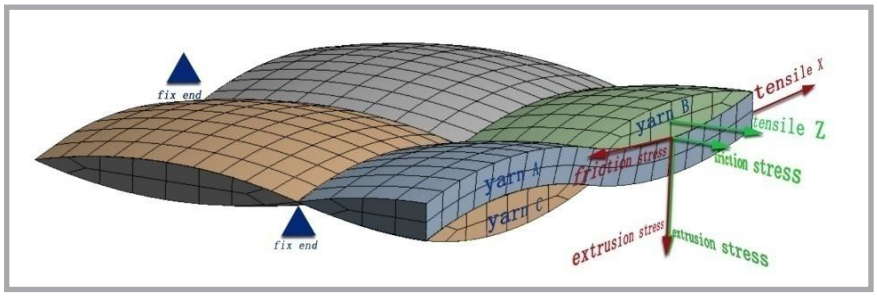


***Figure 15.*** *Stress between yarns in the cross-section of UCPW at the central contact nodal point of yarn A under biaxial tensile loading.*

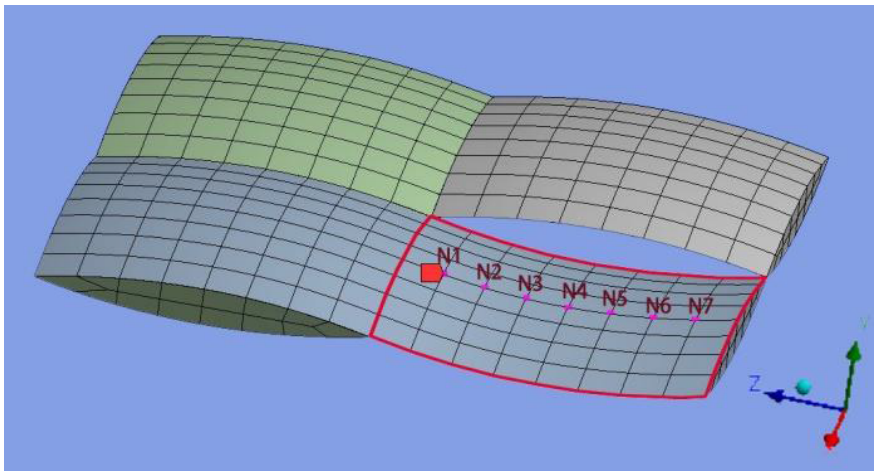


***Figure 16.*** *Positions of N1 to N7 in the UCPW and single yarn at a crimprate of 3.341%.*

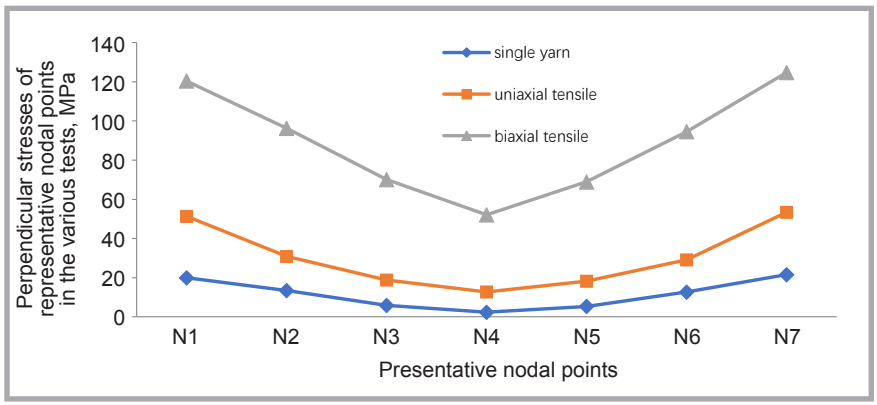


***Figure 17.*** *Perpendicular stresses (MPa) at representative nodal points in the various tests at the same crimp – 3.341% and inter-yarn frictional coefficient – 0.3.*

sile test than in the uniaxial test. As in the uniaxial case, the distribution of the moduli had the same downward trend. The equivalent modulus of the UCPW dropped from 99.79% to 97.08% of the original modulus when the crimp increased from 1.167% to 4.658%. Therefore, at the same crimp and inter-yarn friction coefficient, the equivalent modulus was greater in the biaxial tensile test than in the uniaxial test. The linear fitting results also reveal that the crimp had slightly less influence in the case of the biaxial tensile test than in the uniaxial test.

From a microscopic perspective, as tensile loading was applied to the yarns in the warp and weft directions, the stress situation was much more complicated in the biaxial test than in the uniaxial case, as shown in ***Figure 15***. For example, at the central contact nodal point of yarn A, the tensile load in the x direction (tensile x in the schematic) was applied directly to yarn A. As in the uniaxial case, tensile elongation resulted in friction stress on the contact surface caused by the hindrance of yarns B and C; simultaneously, the bending of yarn A also resulted in extrusion stress normal to the fabric plane on the contact surface due to the hindrance of yarns B and C. In addition, another tensile load was applied to yarns B and C in the z direction. Owing to symmetry, only yarn B was taken into consideration. The tensile elongation of yarn B resulted in friction stress on the contact surface of A, and the bending of yarn B also resulted in extrusion stress on yarn A. Therefore, it is obvious that both friction stress and extrusion stress at the nodal points of the contact area were greater compared with the uniaxial case. In the following analysis, we will discuss the quantification of inter-yarn friction.

Generally, regardless of the type of tensile test (single yarn, uniaxial, or biaxial), the equivalent modulus gradually decreases as the crimp of the yarn increases. Furthermore, at the same level of crimp, the equivalent modulus of the UCPW decreases in the following order: biaxial test, uniaxial test, single yarn test.

**Effect of inter-yarn friction on the mechanical behaviour of UCPW**

Typically, the compressive stress generated on the contact surface and the contact friction coefficient are the two main factors affecting the friction force, and under the same objective condition, the friction force between yarns in the fabric is supposed to have an influence on the fabric's tensile properties. Therefore, in the present study we attempted to determine the effect of inter-yarn friction on a fabric's tensile properties from the perspective of both the contact stress and friction coefficient, as well as to elucidate the underlying mechanism.

***Investigation of contact stress***

The inter-yarn friction force in fabrics is very difficult to calculate [24]. However, the greater the pressure between the contact surfaces, the greater the friction force generated. Therefore, the variation in the friction force can be determined by measuring the change in the contact pressure. From a microscopic perspective, the frictional force of each affected FE nodal point is determined by the normal contact stress. In the present study, we chose the cyclic contact area highlighted by the surrounding red line in the UCPW shown in ***Figure 16***. We selected seven representative nodal points on the surface of a certain yarn and designated them $N_1$ to $N_7$, then examined and compared the stresses at these seven nodal points. Because the model is symmetrical, the stresses at these representative nodal points basically represent those of the whole yarn or UCPW. We examined the perpendicular stresses (in the y direction, perpendicular to the fabric plane) to determine the extrusion pressure between the contact area of the yarn. At the same crimp of 3.341%, and inter-yarn frictional coefficient of 0.3, we investigated the three tests (single yarn, uniaxial, and biaxial tensile) at the same representative nodal points. The perpendicular stresses at $N_1$ to $N_7$ in the different tests are given in ***Figure 17***.

In a tensile process involving a single yarn, perpendicular stress is caused by the bending of the yarn, as mentioned above, whereas in uniaxial or biaxial tensile processes, in addition to bending, the mutual extrusion interaction in the contact area of the yarn caused by tensile loading also contributes to perpendicular stress. ***Figure 17*** demonstrates that during tensile processes, the perpendicular stresses at the representative points in a single yarn,

which are mostly caused by bending, are quite small compared with those in the UCPW (approximately 12.5% of the perpendicular stress in the biaxial case and 36.8% in the uniaxial case). In other words, bending only accounts for a small part of the stress compared with the mutual extrusion between yarns. In the UCPW tensile test, the mutual extrusion between contact yarns was responsible for most of the perpendicular stress. In the single yarn tensile case, the perpendicular stress was quite small because there was no inter-yarn contact; whereas in the UCPW case, the yarn protruded from the deformation as a result of tensile loading, and the deformation in the biaxial case was greater than in the uniaxial case because multiple loading was applied. This led to greater mutual extrusion stress in the biaxial test than in the uniaxial test. Under the same friction coefficient, the greater the interaction pressure between yarns, the greater the friction produced during a tensile process. Therefore, under biaxial tension, more protruding deformation causes more contact stress, resulting in greater friction. According to the statistical analysis of the representative nodal points, the perpendicular stress in the biaxial case was on average 2.86 times greater than in the uniaxial case, and 7.93 times greater than in the single yarn. At the same crimp, a larger friction force leads to larger internal stress in the yarns, which makes them more difficult to stretch, resulting in a larger equivalent modulus than during uniaxial tension. This provides a good explanation as to why the equivalent modulus of the UCPW varied in the single yarn, uniaxial and biaxial tensile processes.

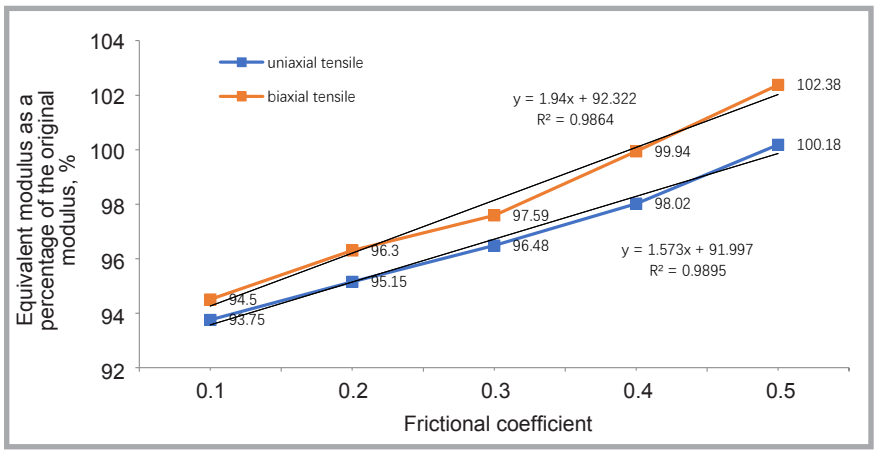


***Figure 18.*** *Equivalent modulus as a percentage of the original modulus versus the inter-yarn frictional coefficient in UCPW under tensile loading.*

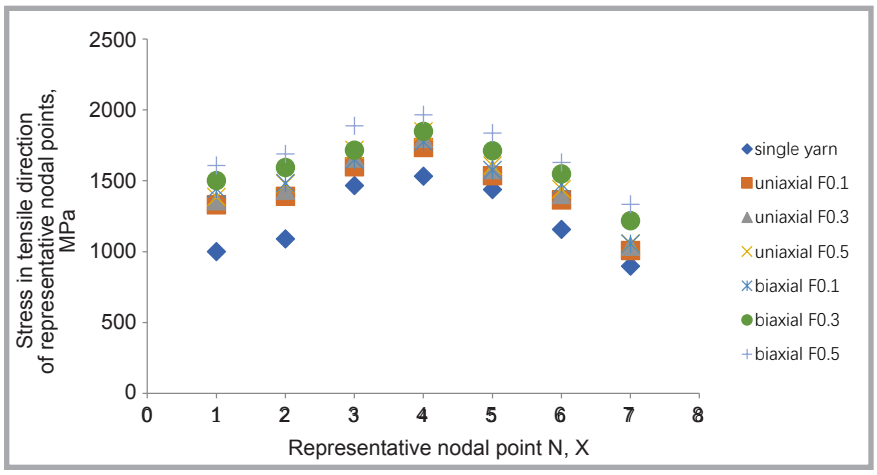


***Figure 19.*** *Comparison of stress at representative nodal points in the tensile direction for the various tests.*

### *Effect of inter-yarn friction coefficient*

Inter-yarn friction is another important factor that influences the mechanical properties of a fabric. At the same crimp rate and tensile elongation, a larger friction coefficient results in a greater friction force between two contact yarns during tensile loading. A greater friction force contributes to greater internal stress in the yarn during loading, as mentioned above, which further influences the tensile properties. We were most concerned with how and to what extent the inter-yarn friction coefficient affects the equivalent modulus during tensile processes. Therefore, we used the same UCPW at the same crimp rate of 3.341% in both the uniaxial and biaxial tensile tests. We applied five friction coefficients (0.1, 0.2, 0.3, 0.4 and 0.5) to the contact boundary condition, the results of which are shown below.

***Figure 18*** shows that the equivalent modulus increased along with the frictional coefficient. Increasing the inter-yarn friction raises the friction force during the tensile process, and this leads to stronger resistance, resulting in an increase in the equivalent modulus. Furthermore, the results show that the equivalent modulus was greater than the original modulus when the friction coefficient reached 0.5 in both tensile cases. Therefore, the equivalent modulus may be larger than the original modulus when the inter-yarn friction is large enough. Moreover, under certain mechanical conditions and at a certain inter-yarn friction, it is possible for the equivalent modulus of a fabric to be the same as the original modulus.

***Figure 19*** shows the stresses in the tensile direction (z) at the representative nodal points at a crimp of 3.341% in the single yarn in biaxial and uniaxial tensile cases at friction coefficients of 0.1, 0.3, and 0.5. The results reveal the following: First, the stress in the single yarn case was lowest at all points because there was no inter-yarn friction. Second, in both the biaxial and uniaxial tests, the stress in the tensile direction became noticeably higher when the friction coefficient increased, owing to the higher friction force between the yarns. According to the statistical analysis of the representative nodal points, the stress in the tensile direction in the biaxial and uniaxial tests increased by 19.3% and 8.8% on average, respectively, when the frictional coefficient varied from 0.1 to 0.5. Third, at the same friction coefficient, the stress was higher in the biaxial case than in the uniaxial case. According to the statistical analysis of the representative nodal points, the stress in the tensile direction was 24.2% larger on average in the biaxial test than in the uniaxial test, which also explains why the equivalent modulus in the biaxial case was higher than in the uniaxial case at the same crimp and friction coefficient.

## Conclusions

In the present paper, we investigated how and to what extent the physical characteristics of a fabric influence its mechanical properties during tensile processes. Firstly, an FE model of plain weave was created and proved to be effective compared to the tensile experiment with Twaron CT® plain weave fabric. Secondly, tensile simulations representing a single yarn, as well as uniaxial and biaxial UCPWs were carried out considering different yarn crimp rates. Regardless of the tensile test (single yarn, uniaxial, or biaxial), the equivalent modulus gradually decreases as the crimp of the yarn increases. Furthermore, at the same level of crimp, the equivalent modulus decreases in the following order: biaxial test, uniaxial test, single yarn test. We chose representative nodal points, and investigated and analysed the deformation and normal stress. The results revealed that in the case of a single yarn, greater crimp will have greater displacement, caused by bending during the tensile process, and unstable dynamic action reduces the tensile stress in the tensile direction. In other words, the bigger the crimp, the easier it is to stretch the yarn, which has a smaller equivalent modulus. Moreover, we determined why there was a difference in the equivalent modulus between the single yarn, uniaxial, and biaxial tensile tests by investigating the stress at the representative inner nodal points. Thirdly, we considered the influence of inter-yarn friction. We analysed the contact stresses in a group of nodal points chosen in the model, and the results showed that under biaxial tension, more protruding deformation causes more contact pressure, producing a larger friction force. At the same crimp, a larger friction force leads to larger internal stress in the yarns, which makes them more difficult to stretch, resulting in a larger equivalent modulus than during uniaxial tension. We then carried out tensile tests on UCPWs with different inter-yarn frictional coefficients at the same crimp rate. The stresses in the tensile direction at the representative nodal points were also investigated. There was an obvious tendency for the equivalent moduli of the UCPWs to increase as the frictional coefficient increased in both the uniaxial and biaxial tensile tests.

## References


1. Mahadik Y*, Hallett SR. Finite Element Modeling of Tow Geometry in 3D Woven Fabrics. *Composites: Part A* 2010; 41; 1192-1200.
2. Tehrami-Dehkordi M, Nostray H. Tensile Behavior Simulation of Woven Fabric with Different Weave Pattern Based on Finite Element Method. *Journal of Textiles and Polymers* 2015; 3.
3. Lin J J. Applying GM to Predicting Elastic Property and FEM to Analyzing Tensile Damage Behavior for Woven Fabric. *J. Text. Inst.* 2014; 105: 1029-1041.
4. Chen S, Ding X, Fangueiro R, Yi H, Ni J. Tensile Behavior Of PVC-Coated Woven Membrane Materials Under Uni- and Bi -Axial Loads. *J Appl Polym Sci* 2008; 107: 2038-44.
5. Lin H, Long AC, Sherburn M, Clifford M J. Modelling of Mechanical Behaviour for Woven Fabrics Under Combined Loading. *International Journal of Material Forming* 2008; 4: 899–902.
6. Manohar G. Kollegal, Srinivasan Sridharan. Strength Prediction of Plain Woven Fabrics. *Journal of Composite Materials* 2000, 34(3): 240-257.
7. Wu J, Pan N. Grab and Strip Tensile Strengths for Woven Fabrics: An Experimental Verification. *Text Res J*. 2005; 75: 789-96.
8. Leaf G A V, Kandil K H. The Initial Load -Extension Behaviour of Plain Woven Fabrics. *J. Text. Inst*., 1980; 71: 1-7.
9. Reinhardt HW. On the Biaxial Testing and Strength of Coated Fabrics. *Exp Mech* 1976; 16(2): 71-4.
10. Chen S, Ding X, Yi H. On the Anisotropic Tensile Behaviors of Flexible Polyvinyl Chloride-Coated Fabrics. *Text Res J*. 2007; 77(6): 369-74.
11. Zhang Y, Zhang Q, Ke L, Bei-lei K. Experimental Analysis of Tensile Behaviours of Polytrafluoroethylene-Coated Fabrics Subjected to Monotonous and Cyclic Loading. *Text Res J*. 2014; 84(3): 231-45.
12. Majid Tehrani-Dehkordi, Hooshang Nosraty. Tensile Behavior Simulation of Woven Fabric with Different Weave Pattern Based on Finite Element Method. *Journal of Textiles and Polymers* 2015; 3(1) 1: 34-39.
13. Tan VBC, Shim VPW, Zeng X. Modelling Crimp in Woven Fabrics Subjected to Ballistic Impact. *Int J Impact Eng* 2005; 32: 561-74.
14. Ying Wang, Xiaogang Chen, Robert Young, Ian Kinloch. Finite Element Analysis of Effect of Inter-Yarn Friction on Ballistic Impact Response of Woven Fabrics. *Composite Structures* 2016; 135: 8-16.
15. Broughton Roy M, Yehia El Mogahzy, Hall D M. Mechanism of Yarn Failure. *Textile Research Journal* 1992; 62( 3): 131-134.
16. Youqi Wang, Yuyang Miao, Lejian Huang, Daniel Swenson, Chian-Fong Yen, Jian Yu, James Zheng. Effect of the Inter-Fiber Friction on Fiber Damage Propagation and Ballistic Limit Of 2-D Woven Fabrics Under A Fully Confined Boundary Condition. *International Journal of Impact Engineering* 2016; 97: 66-78.
17. Yanyan Chu, Shengnan Min, Xiaogang Chen. Numerical Study of Inter-Yarn Friction on the Failure of Fabrics Upon Ballistic Impacts. *Materials and Design* 2017; 115: 299-316.
18. Ying Wang, Xiaogang Chen, Robert Young, Ian Kinloch. A Numerical and Experimental Analysis of the Influence of Crimp on Ballistic Impact Response of Woven Fabrics. *Composite Structures* 2016; 140: 44-52.
19. Gogineni S, Gao X-L, David NV, Zheng JQ. Ballistic Impact of Twaron CT709® Plain Weave Fabrics. *Mechanics of Advanced Materials and Structures* 2012; 19, 6: 441-452.
20. Lim CT*, Shim VPW, Ng YH. Finite-Element Modeling of the Ballistic Impact of Fabric Armor. *International Journal of Impact Engineering* 2003; 28: 13-31.
21. Gasser A, Boisse P, Hanklar S. Mechanical Behavior of Dry Fabric Reinforcement. 3D Simulations Versus Biaxial Tests. *Comput. Mater. Sci.* 1999; 17, 7-20.
22. López-Gálvez H, Rodriguez-Millán M, Feito N, Miguelez H. A Method for Inter-Yarn Friction Coefficient Calculation for Plain Wave of Aramid Fibers. *Mechanics Research Communications* 2016; 74: 52-56.
23. Carvelli V, Poggi C. A Homogenization Procedure for the Numerical Analysis of Woven Fabric Composites. *Composites Part A: Applied Science and Manufacturing* 2001; (32): 1425-1432.
24. Frącczak Ł, Matusiak M, Zgórniak P. Investigation of the Friction Coefficient of Seersucker Woven Fabrics. *FIBRES & TEXTILES in Eastern Europe* 2019; 27, 3(135): 36-42. DOI: 10.5604/01.3001.0013.0740.


***Received 17.02.2020 Reviewed 14.05.2020***